UNIVERSITY OF BATH

Citation for published version:
Enang, W, Bannister, C, Brace, C & Vagg, C 2015, 'Modelling and heuristic control of a parallel hybrid electric vehicle', *Proceedings of the Institution of Mechanical Engineers, Part D: Journal of Automobile Engineering*, vol. 229, no. 11, pp. 1494-1513. https://doi.org/10.1177/0954407014565633

DOI:
10.1177/0954407014565633

Publication date:
2015

Document Version
Peer reviewed version

Link to publication

Enang, Wisdom ; Bannister, Chris ; Brace, Chris ; Vagg, Chris. / Modelling and heuristic control of a parallel hybrid electric vehicle. In: Proceedings of the Institution of Mechanical Engineers, Part D: Journal of Automobile Engineering. 2015 ; Vol. 229, No. 11. pp. 1494-1513. (C) IMechE 2015. Reprinted by permission of SAGE Publications.

University of Bath

Alternative formats
If you require this document in an alternative format, please contact:
openaccess@bath.ac.uk

General rights
Copyright and moral rights for the publications made accessible in the public portal are retained by the authors and/or other copyright owners and it is a condition of accessing publications that users recognise and abide by the legal requirements associated with these rights.

Take down policy
If you believe that this document breaches copyright please contact us providing details, and we will remove access to the work immediately and investigate your claim.

Download date: 05. May. 2023

Modelling and Heuristic control of a Parallel Hybrid Electric Vehicle

Wisdom Enang [1*], Chris Bannister [1], Chris Brace [1], Chris Vagg [1]

(1) University of Bath, Bath, UK
(*) Corresponding Author (wpe20@bath.ac.uk)

ABSTRACT

Hybrid electric vehicles (HEVs) offer the potential for fuel consumption improvements when compared to conventional vehicle powertrains. The fuel consumption benefits which can be realised when utilising HEV architecture are dependent on how much braking energy is regenerated, and how well the regenerated energy is utilized.

A number of power management strategies have been proposed in literature. Owing to the prospect of real time implementation, much of these proposals have centred on the use of heuristics. Despite the research advances made, the key challenge with heuristic strategies remain achieving reasonable fuel savings without over depleting the battery state of charge at the end of the trip.

In view of this challenge, this paper offers 2 main contributions to existing energy management literature. The first is a novel, simple but effective heuristic control strategy which employs a tuneable parameter (percentage of maximum motor tractive power) to decide the control sequence, such that impressive fuel savings are achieved without over depleting the final battery state of charge (battery energy). The second is the quantitative exploration of braking patterns and its impact on kinetic energy regeneration.

The potential of the proposed heuristic control strategy was explored over a range of drive cycles which reflect different driving scenarios. Results from this analysis show, that as much as 19.07% fuel savings could be achieved over the JAPAN1015 drive cycle. In comparison to a suboptimal controller whose control signals were derived from dynamic programming optimal control, our proposed strategy was found to be outperforming, in that it achieved impressive real time fuel savings without much penalty to the final battery state of charge. Gentle braking patterns were also found to significantly improve brake energy regeneration by the electric motor.

Index Terms: - Heuristic control, Hybrid electric vehicle, Gear shift strategy, Regenerative braking, Optimization of brake energy recovery, dynamic programming, optimal control, HEV control, vehicle modelling, Parallel HEV.

1 INTRODUCTION

Increased prices of fossil fuels and shortages of world fuel reserves have created an eminent and urgent need for the production of automobiles with improved fuel economy [1, 2], [3]. One of such emerging technology is that of the hybrid vehicle. Hybrid vehicles generally refer to vehicles fitted with more than one type of energy converter and energy storage for its propulsion. Energy converter options currently in use in hybrid systems today include, heat engines, hydraulic engines and electric motors. One important reason for introducing hybrid vehicle systems, is to improve fuel economy and emissions. In the hybrid electric vehicle system which includes electric motors, this objective is achieved mainly by regenerating the brake energy of the vehicle for future use in vehicle accelerations and engine assist.

Accurate modelling and control is essential to maximizing the fuel saving potential of the hybrid electric vehicle power train. Three possible approaches exist for HEV modelling at the detailed modelling stage of the development process: the kinematic or backward approach, the quasi static or forward approach, and the dynamic approach [4].

The kinematic approach is a backward methodology where the input variables are the speed of the vehicle and the grade angle of the road. In this method, the engine speed is being determined using simple kinematic relationships starting from the wheel revolution speed and the total

transmission ratio of the driveline. The tractive torque that should be provided to the wheels to drive the vehicle according to the chosen speed profile can be calculated from the main vehicle characteristics e.g. (vehicle mass, aerodynamic drag and rolling resistance). The calculated engine torque and speed is then used alongside with a statistical fuel consumption model to make an instantaneous fuel consumption or emissions rate prediction [4]. The kinematic approach makes the assumption that the vehicle meets the target performance, so that the vehicle speed is supposed known a priori; thus enjoying the advantage of simplicity and low computational cost [5]. The backward or kinematic modelling method ensures that the driving speed profile will be exactly followed, on the other hand there exist no guarantees that the given vehicle will actually be able to meet the desired speed trace, since the power request is directly computed from the speed and not checked against the actual power train capabilities. Another flaw of this modelling technique is its negligence of thermal transient behaviour of engines which are noticeable after an engine cold start.
The simplification of transient conditions as a sequence of stationary states limits this modelling method to an option considerable mainly for preliminary estimation of vehicle fuel consumption and emissions [6].

The quasi static approach of HEV modelling makes use of a driver model typically a PID which compares that target vehicle speed (drive cycle speed), with the actual speed profile, of the vehicle and then generates a power demand profile which is needed to follow the target vehicle speed profile. This power demand profile is generated by solving the differential motion equation of the vehicle [5]. Once the propulsion torque and speed of the engine have been determined, instantaneous fuel consumption can be estimated using a statistical engine model as already explained in the kinematic or backward approach. The suitability and accuracy of the quasi-static modelling approach depends very much on nature of simulation studies to be conducted. The quasi-static modelling approach provides reasonable accuracy when it comes to the evaluation of the fuel consumption and NOx of a vehicle equipped with conventional power train. For pollutants like soot, the acceleration transients and related “turbo-lag” phenomena significantly contribute to the cycle cumulative emissions, thus necessitating a more detailed engine simulation model which is capable of properly capturing engine transient behaviour in more details [7].

In the dynamic modelling approach, the internal combustion engine behaviour during transients is also modelled in addition to the longitudinal vehicle dynamics. The engine transient behaviour is modelled by means of a detailed one dimensional fluid dynamic model. For example the intake and exhaust systems of the internal combustion engine in the dynamic modelling approach are represented as a network of ducts connected by the junctions that represent either physical joints between the ducts, such as area changes or volumes or subsystems such as the engine cylinder. Solutions to the equations governing the conservation of mass, momentum and energy flow for each element of the network can then be obtained using a finite difference technique. This makes it possible for highly dynamic events such as abrupt vehicle accelerations to be properly and reliably simulated with reasonable accuracy. The implementation of dynamic modelling comes with a huge time and computational burden and as such its application is often limited to research areas which deal with internal combustion engine development [8], [9], [10].

Hybridization brings about the question of how to co-ordinate the on-board power sources in order to maximize fuel economy and reduce emissions. HEV power management strategies could be broadly classified in to optimization based methods that control the power split using exact knowledge of the vehicle power demand, and rule based real time implementable methods, which control the power split without exact knowledge of the future vehicle power demand.

Optimization based control strategies decide the control signals either by minimizing the sum of the objective function over time (global optimization) or by instantaneously minimizing the objective function (local optimization). Dynamic programming [11-17], ECMS (equivalent consumption minimization strategy) [18-22] and PMP (Pontryagin minimum principle) [23, 24] have all been applied as optimization techniques for HEV optimal energy management.

Dynamic programming, originally developed by Richard Bellman, solves discrete multi-stage decision problems by selecting a decision based on the optimization criterion from a finite number of decision variables at each time step. ECMS and PMP alike are special cases of the Euler-Lagrange equation of variational calculus, which characterizes the equivalent fuel for electrical energy consumption. While useful in identifying the ultimate fuel saving potential of an HEV over a drive cycle, these approaches are not suitable for real time implementation in their original form, as they are time consuming and require

information about the vehicle's future power demand before the trip, which is clearly infeasible.

Variations to the ECMS optimization control strategy have been reported by a number of studies and shown to be implementable in real time. Some of such variations include the Adaptive ECMS [25, 26] and Telemetry ECMS [27], which adjust the equivalent factor based on past driving data and future prediction. The downside to these adaptive techniques however, is the need for predictive equipment like GPS (global positioning system) which often constitutes additional cost.

Heuristic strategies in comparison, are easily implementable in real time and with the potential for simplicity, customization and robustness; they have been reported to show a near optimal performance if the rules are made detailed enough to take care of any special event that may affect the vehicle [2, 28-33].

Recent advances in heuristic controller research have focused on the use of fuzzy logic, in which linguistic representation of the control inputs are converted in to numerical representation with membership functions in the fuzzification and defuzzification process. Schouten *et al.* [34] using the fuzzy logic technique, developed a fuel optimization control strategy for parallel HEVs which was based on the efficiency optimization of different parts of the vehicle (engine, electric motor and battery). Adaptive fuzzy control strategy is becoming increasingly popular in automotive application, because it creates the possibility for simultaneous optimization of fuel efficiency and emissions. An application of adaptive fuzzy logic controllers in solving conflicting objective control problems involving NOx, CO and HC emissions, have been reported in literature [35, 36].

Despite these research advances, heuristic controllers still suffer massively from over depletion of battery state of charge at the end of the drive cycle. In view of this problem, a simple but effective heuristic control strategy which employs a "switch parameter" for power split is proposed and tuned over 3 standard drive cycles, to ensure that real time fuel savings are achieved whilst avoiding over depletion of the final battery state of charge.

The layout of this paper is outlined as follows: first a quasi-static modelling approach is used to mathematically represent our vehicle, after which the simulated baseline fuel consumption profile of the model is validated against the experimental fuel consumption profile of the actual vehicle. Next, the proposed heuristic control strategy is developed and its performance is benchmarked against that of the dynamic programming optimal control strategy and that of a suboptimal control strategy whose control rules are extracted from the optimal controller. Finally, the impact of braking patterns on kinetic energy regeneration is investigated.

2 HEV POWERTRAIN MODELLING

In a control application where reduction in fuel consumption is the primary objective, it is important to develop vehicle models with a robust and accurate ability to predict fuel consumption even under rapid transients. This section will compose mainly of the physical and mathematical modelling of a parallel hybrid electric vehicle in a Matlab/Simulink environment. The vehicle subsystems detailed in this section aim to model to a high level of accuracy the vehicle components which significantly affect fuel consumption.

2.1 Description of drive train architecture

The parallel hybrid electric vehicle drive train to be modelled is introduced in Figure 1.

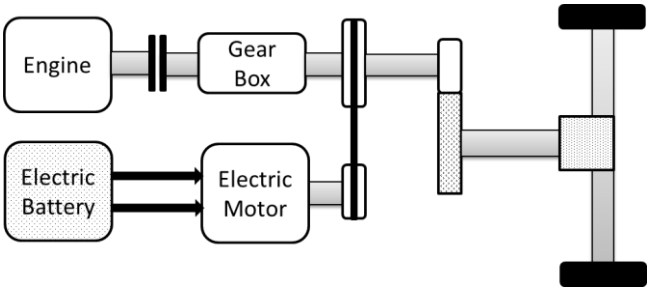

Figure 1: Parallel hybrid electric vehicle

Data used in modelling the HEV presented in this paper is detailed in Appendix 1.

The HEV configuration employed in this vehicle permits the following modes of operation as shown in Figure 2.

1. Regenerative braking
2. Power assist
3. Motor only
4. Trickle charge
5. Engine only

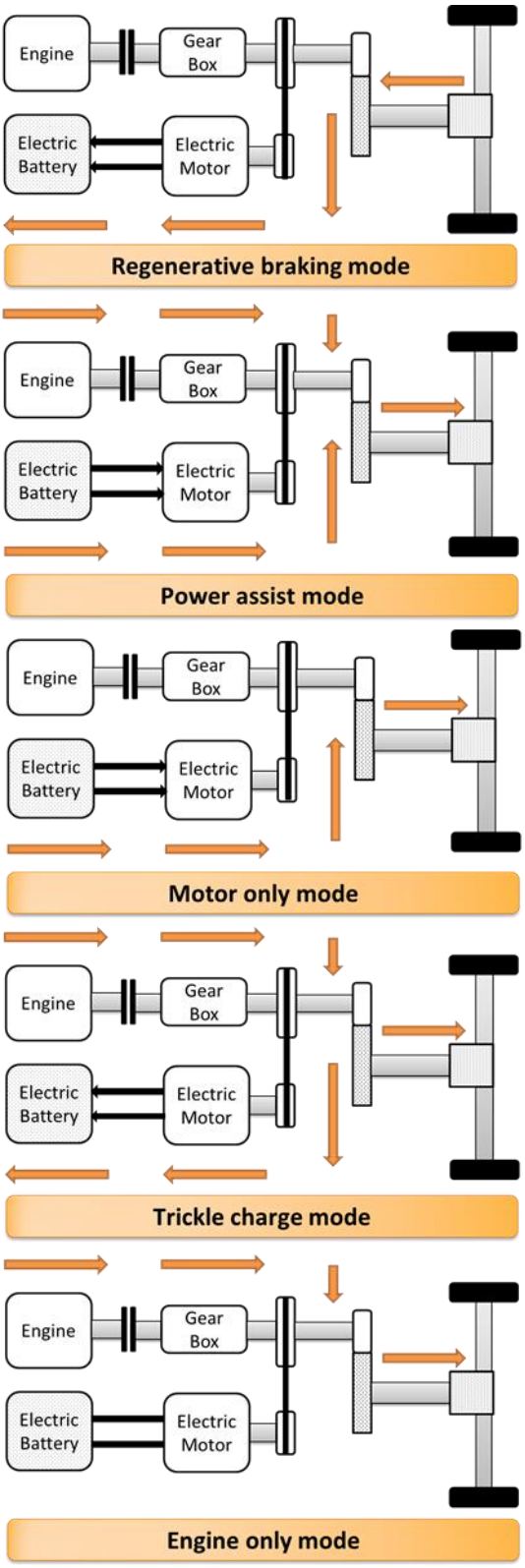

Figure 2: HEV operating modes with power flow

In the regenerative braking mode, the HEV uses the electric motor to recover kinetic braking energy which would otherwise have been lost as heat to the mechanical brakes. The captured braking kinetic energy is converted to electrical energy and stored in the battery for use during the motor only mode or power assist mode.

In the power assist HEV mode, the electric motor operates to assist the engine in regions of low engine efficiency or high vehicle power demand.

In the motor only mode, the HEV operates mainly as an electric vehicle, in which case the engine is disengaged from the drive train by means of a clutch and allowed to idle. Operating the HEV in this mode means that the entire energy which drives the drivetrain comes from the batteries.

In the trickle charge mode, the engine is used to drive the road load, maintain the drive cycle speed request, as well as recharge the batteries via the electric motor. Operating an HEV in this mode imposes an extra cost (fuel consumption) on it, which is one of the reasons why such practice is strongly discouraged, except on occasions where the battery SOC (state of charge) has dropped below the recommended lower bound and needs to be brought back up to at least its lower bound so as to avoid damaging the battery cells.

In the Engine only mode, the HEV load and speed request are met solely by the internal combustion engine.

2.2 Driver modelling

The driver in this HEV model is designed as a simple PID controller with the addition of an anti-windup on the Integrator. At each simulation time, the extra wheel torque needed for the vehicle to achieve the required vehicle speed is calculated as shown in equation 1:

$$T_{extra} = K_p(V_c - V_v) + K_i \int (V_c - V_v)\, dt + K_d \frac{d(V_c - V_v)}{dt} \quad (1)$$

From equation 1, the extra tractive force needed for the vehicle to achieve the required vehicle speed could be calculated thus:

$$F_{extra} = \frac{T_{extra}}{R_w}$$

The gain values of the PID controller were tuned using parameter estimation in MATLAB to find the values which best enables the vehicle follow the required speed-time trace. The values obtained from tuning are: $K_p = 0.272$, $K_i = 0.35$, $K_d = 2$. The PID driver model's ability to follow the required vehicle speed trace is shown below in Figure 3

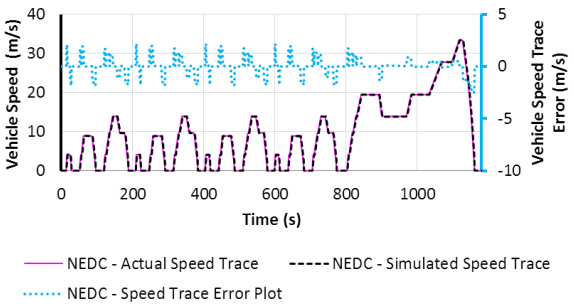

(a) NEDC drive cycle profile

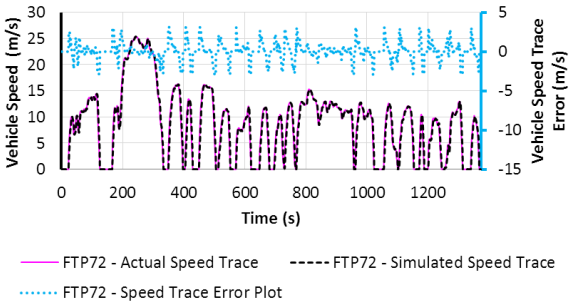

(b) FTP72 drive cycle profile

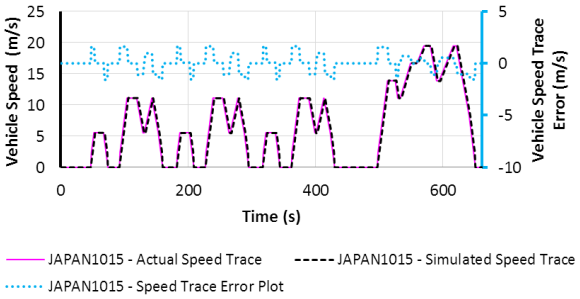

(c) JAPAN1015 drive cycle profile

Figure 3: PID driver tracking ability over the NEDC, FTP72 and JAPAN1015 drive cycle

The PID driver model is shown to command good track ability over the NEDC, FTP72 and JAPAN1015 drive cycles as shown in Figure 3(a) to Figure 3(c) respectively, despite the high level of aggressive driving characteristics which make up the FTP72 drive cycle.

2.3 Vehicle dynamics modelling

For the purpose of a control strategy development, a simple mechanical and mathematical model representing the longitudinal performance of the vehicle is required.

The first and fundamental step in modelling the dynamics of any vehicle is to obtain the relevant road load equation which characterizes the vehicle propulsion. The frictional force, aerodynamic force and grade force all make up the road load we wish to characterize.

When a vehicle is in forward motion, the movement produced by the forward shift of the ground reaction force is called the rolling resistance moment which could be expressed thus:

$$T_{rolling} = \mu N_c R_w \quad (2)$$

To keep the wheel rolling, a force: $F_{rolling}$ acting through the centre of the wheel is required to balance the rolling resistance moment [37], [38]. This force could be expressed thus:

$$F_{rolling} = \mu N_c \quad (3)$$

The coefficient of rolling resistance μ is a function of the tyre material, tire structure, tire temperature, tire inflation pressure and tire geometry.

A vehicle travelling at a particular speed in air encounters a force resisting its motion. This force known as aerodynamic force, results mainly from two components: shape drag and skin friction [37], [38], [39].

Aerodynamic force (F_{aero}), is a function of the vehicle speed, vehicle frontal area, air density and coefficient of air drag. The aerodynamic force could be expressed mathematically thus:

$$F_{aero} = 0.5\rho A_f C_d (V_v - V_a)^2 \quad (4)$$

As a vehicle goes up or down a slope, its weight produces a component load, which is always directed in to the downward direction. This component load either opposes the forward motion (grade climbing) or helps the forward motion (grade descending).

The grade resistance could be expressed thus:

$$F_{grade} = mg\sin(\beta) \quad (5)$$

Combining the vehicle loads derived thus far in accordance to Newton's second law, the engine torque and speed, could be expressed thus for a parallel hybrid electric vehicle:

$$T_{ICE} = \frac{(m\frac{dV_v}{dt} + \sum(F_{aero} + F_{rolling} + F_{grade} + F_{extra}))R_w}{FDR\ G_E\ Eff} - \frac{T_{motor}\ G_M}{G_E} \quad (6)$$

Where: $T_{motor} = \frac{P_{motor}}{G_M\ FDR\ W_{wheel}\frac{2\pi}{60}}$

The engine torque demand expressed in equation 6 could be further expressed thus:

$$T_{ICE} = \frac{(m\frac{dV_v}{dt} + \sum(F_{aero} + F_{rolling} + F_{grade} + F_{extra}))R_w}{FDR\ G_E\ Eff} - \frac{P_{motor}}{G_E\ FDR\ W_{wheel}\frac{2\pi}{60}} \quad 7$$

The general engine speed equation could be expressed thus:

$$W_{ICE} = W_{wheel}\ FDR\ G_E\ \frac{2\pi}{60} \quad 8$$

2.4 Engine modelling

Engine modelling in the development of an HEV control strategy centres mainly on the use of mathematical and statistical methods to accurately predict the objective function to be minimized (fuel consumption).

During the operation of this parallel HEV, the engine is only a functional part of the power train during the following operating modes: the power assist mode, trickle charge mode and the engine only mode. This means that the engine idles when not in use. During braking, no fuel is however injected in to the engine.

Fuel consumption could be expressed as a function of engine torque and engine speed as shown in Figure 4.

Using the engine torque and speed values derived from equation 7 and equation 8 respectively, the instantaneous fuel consumption rate for each engine torque-speed point could be read off the "Engine fuel consumption map" detailed in Figure 4. Data used in creating this map was obtained experimentally using the Chassis Dynamometer facility at the University of Bath. Obtaining the engine fuel consumption map in this manner implies that transmission losses have already been accounted for. Consequently, Eff in equation 6 and 7 is taken as 100%.

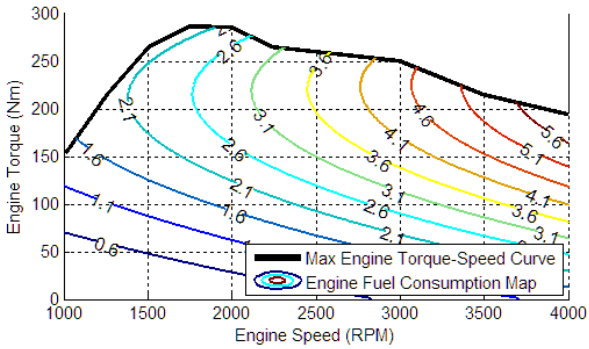

Figure 4: Engine fuel consumption map

2.5 Gear shift strategy

Several ways exist for defining the gear shift over a driving cycle. André et al. [40] pioneered the strategy now known as the "Artermis strategy". This strategy considers simultaneously: the driving condition (engine speed and power demand) and driving styles (database used includes measurement values for various drivers) [41].

The NEDC gear shift strategy performs gear shift on set vehicle speed values. This makes it easy to implement as it depends mainly on vehicle kinematics, however this strategy is only well adapted to steady-speed cycles with few speed transients such as the NEDC drive cycle but is less suitable for real world driving cycles. This is because, in most real world driving cycles the vehicle speed is not steady and often varies around the shift threshold speed, which means that the time spent in a given gear could be very short. Over the NEDC, the gear shift strategy for a 5 speed gear vehicle is defined thus: [41].

0 < V_v(t) < 15 Km/h: ratio = 1
15 < V_v(t) < 35 Km/h: ratio = 2
35 < V_v(t) < 50 Km/h: ratio = 3
50 < V_v(t) < 70 Km/h: ratio = 4
70 < V_v(t): ratio = 5

Where V_v(t) is the vehicle speed (Km/h)

In this paper, a simple "Engine RPM" gear shift strategy is proposed for the vehicle thus:

If RPM(t) > 2000 : ratio(t+1) = ratio(t) + 1 (Upshift)
If RPM(t) < 1000 : ratio(t+1) = ratio(t) – 1 (Downshift)
If V_v(t) = 0 : ratio(t+1) = Neutral
If V_v(t) > 0 : 1 ≤ ratio (t) ≤ 5

This strategy takes in to consideration the vehicle kinematic parameters and the vehicle characteristics in the gearshift pattern. In order to avoid frequent and unrealistic gear change, a minimum 5 seconds delay is imposed on each gear, subject to the engine still being able to provide the vehicle torque requirement at that gear.

Using this gear shift strategy, a sensitivity analysis of the upshift RPM effect on baseline fuel consumption was conducted as shown in Figure 5.

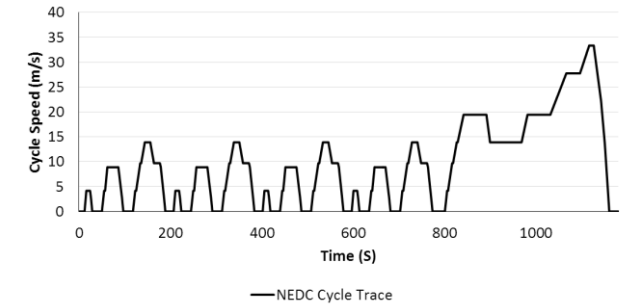

(a) NEDC drive cycle profile

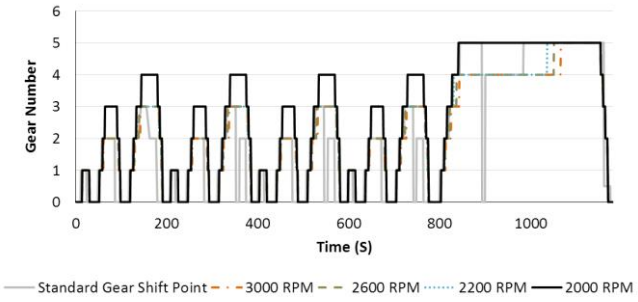

(b) Proposed NEDC gear shift schedule

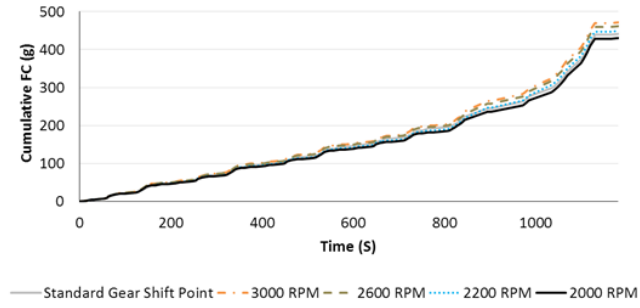

(c) Cumulative fuel consumption profile

Figure 5: Impact of Upshift engine RPM on fuel consumption (NEDC)

This analysis shows a decrease in cumulative fuel consumption (Figure 5(c)) as the upshift engine RPM decreases (Figure 5(b)). Whilst it is evident that a low upshift engine RPM will lead to lower fuel consumption, this advantage must be weighed against driveability constraints such as meeting torque requirements and driver comfort. Comparative to the defined NEDC standard shift strategy, the sensitivity analysis shows that a 2.5% fuel savings could be achieved using an early engine RPM upshift.

The down shift RPM strategy is designed to keep the vehicle driving in the highest possible gear which meets the vehicle torque requirements.

2.6 Electric motor modelling

A wide range of electrical machines are available, depending on the area of application. Generally electric machines could be categorized mainly in to DC and AC machines, synchronous, asynchronous, etc. For the purpose of powertrain control strategy development, electrical machines could be modelled using a system level approach which makes use of a 0D black box model to find the electrical efficiency of the electrical machine at each torque and speed point. The efficiency of the electrical machine η_{motor} is dynamically adjusted with respect to its speed (w_{motor}) and torque (T_{motor}). Depending on the instantaneous motor torque and speed, a look up table is used to estimate the electrical efficiency of the machine.

The electrical power drawn from the battery by the electrical machine could be modelled thus:

$$P_{electric} = \frac{2\pi}{60} P_{motor}\, \eta_{motor} \qquad 9$$

Figure 6 shows the electric motor efficiency map. There exists a maximum torque for both the traction and regeneration performance of the electric motor. This maximum torque varies with motor speed as shown in Figure 6. Data used in creating this map was obtained experimentally and supplied by Perm Motor Germany.

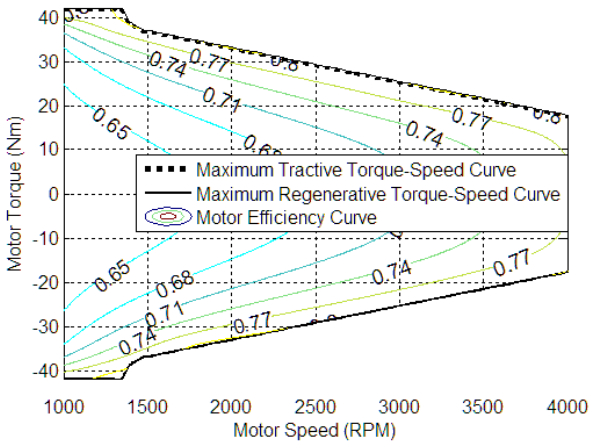

Figure 6: Electric motor efficiency map

2.7 Electric battery modelling

In a typical discharge and charge operation in an HEV, the power flow to and from the battery could be modelled thus:

$$P_{battery}(discharge) = \eta_{dis}\,(+P_{electric}) \quad 10$$

$$P_{battery}(charge) = \eta_{chg}\,(-P_{electric}) \quad 11$$

η_{chg} and η_{dis} is assumed as 80%, which is typical for Lithium ion batteries (Battery modelled in this parallel HEV: see Appendix 1).

The voltage across the battery terminals could be represented mathematically thus:

$$V_{batt} = V_{oc} - IR \quad 12$$

From equation 12, the battery Current (I) and voltage (V_{batt}) could be related to its power using equation 13 below:-

$$P_{battery} = I\,V_{oc} - I^2R \quad 13$$

To derive the battery current, equation 13 could be solved using the quadratic formula to yield:

$$I = \frac{V_{oc}}{2R} - \frac{\sqrt{{V_{oc}}^2 - 4RP_{battery}}}{2R} \quad 14$$

$P_{battery}$: Battery Power (-ve during charging and +ve during discharging).

The battery state of charge (SOC) is a measure of charge left in a battery as a proportion of the maximum possible charge of the battery. In simulation, the battery state of charge is calculated as an integral of battery current (I) over the maximum possible battery charge.

At every simulation time step, the battery state of charge can be calculated thus:

$$SOC_{t+1} = SOC_t \pm \int_t^{t+1} \frac{I}{Q}\,dt \quad 15$$

Charge: (+), Discharge: (-)

2.8 Vehicle model baseline validation

The longitudinal simulation model of our parallel HEV is validated here in this subsection over the NEDC drive cycle as shown in Figure 7. Rather than validating every subsystem in the vehicle, emphasis is laid on validating the vehicle's ability to offer an accurate prediction of the cost function in this case which is fuel consumption.

The experimental data used for the model validation was obtained via an NEDC transient test on a chassis dynamometer with the hybrid system turned off. For the sake of consistency, while obtaining the model validation data, the NEDC standard gear shift points were used both for experimental testing and model simulation.

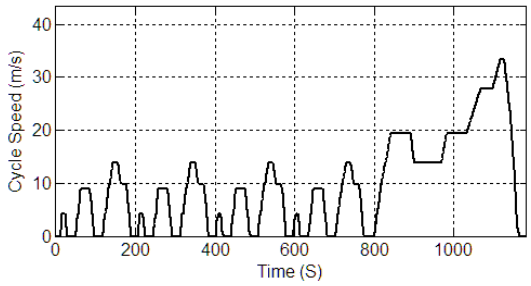

(a) NEDC drive cycle profile

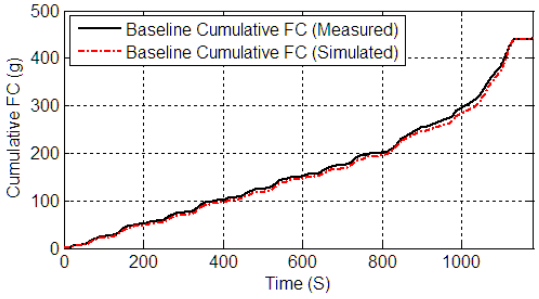

(b) Cumulative fuel consumption validation plot

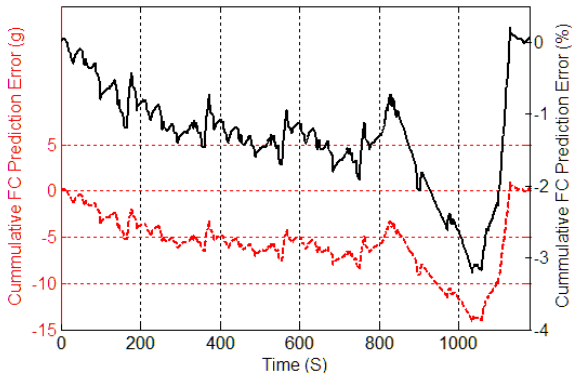

(c) Mass and percentage error in predicted fuel consumption

Figure 7: Model validation over the NEDC drive cycle

As shown in Figure 7(b), the simulated baseline cumulative fuel consumption profile of the vehicle compares very closely to the experimentally obtained profile. A $\pm$3% error range in the model's predictability is observed over the NEDC drive cycle as shown in Figure 7(c).

3 HEURISTIC CONTROL STATEGY SET UP

Heuristic control strategy is the most common way of implementing real time supervisory control in an HEV. The control rules are often based on human intelligence, or mathematical models.

This section aims to outline the implementation of a heuristic power assist control strategy on the parallel hybrid electric vehicle modelled thus far. In this control strategy, the internal combustion engine works as the main source of power, and the electric motor is used to supply a power assist to the engine during periods of high power demand or supply additional power, when power demanded by the vehicle is greater than that which can be supplied by the engine. The electric motor is also used, depending on the battery state of charge, for regenerative braking during braking events. The online implementation of the power assist heuristic control strategy is done using STATEFLOW as will be explained and shown in the upcoming subsections.

Modelling a control strategy with STATEFLOW involves the use of states and transitions to form the basic building blocks of the system. The states of the controller decide the vehicle's operating mode. The transitions are requirements which must be met in order to permit the transition from one vehicle operating mode to the other.

The heuristic control strategy being employed in this controller makes use of a "charge non sustaining" control logic in real time as it does not guarantee the sustainability of the battery state of charge at the end of the drive cycle. However, a lower and upper bound to the battery state of charge has been imposed on the controller to ensure better battery durability. For all simulations, a 60% battery state of charge is used as the initial battery energy level.

3.1 Control logic set up

As shown in Figure 8, the "vehicle power demand" input is used here as the global transition rule which dictates whether the HEV operates in traction mode, braking mode, or simply idles.

The global transition, as defined in Figure 8, could be expressed thus:

If $P_{demand} > 0$ *: Vehicle operates in traction mode*

If $P_{demand} == 0$ *: Vehicle Idles*

If $P_{demand} < 0$ *: Vehicle Operates in braking mode*

Figure 8 also outlines the inter-mode control logic which governs how the electric motor is being utilized both for traction and for regenerative braking.

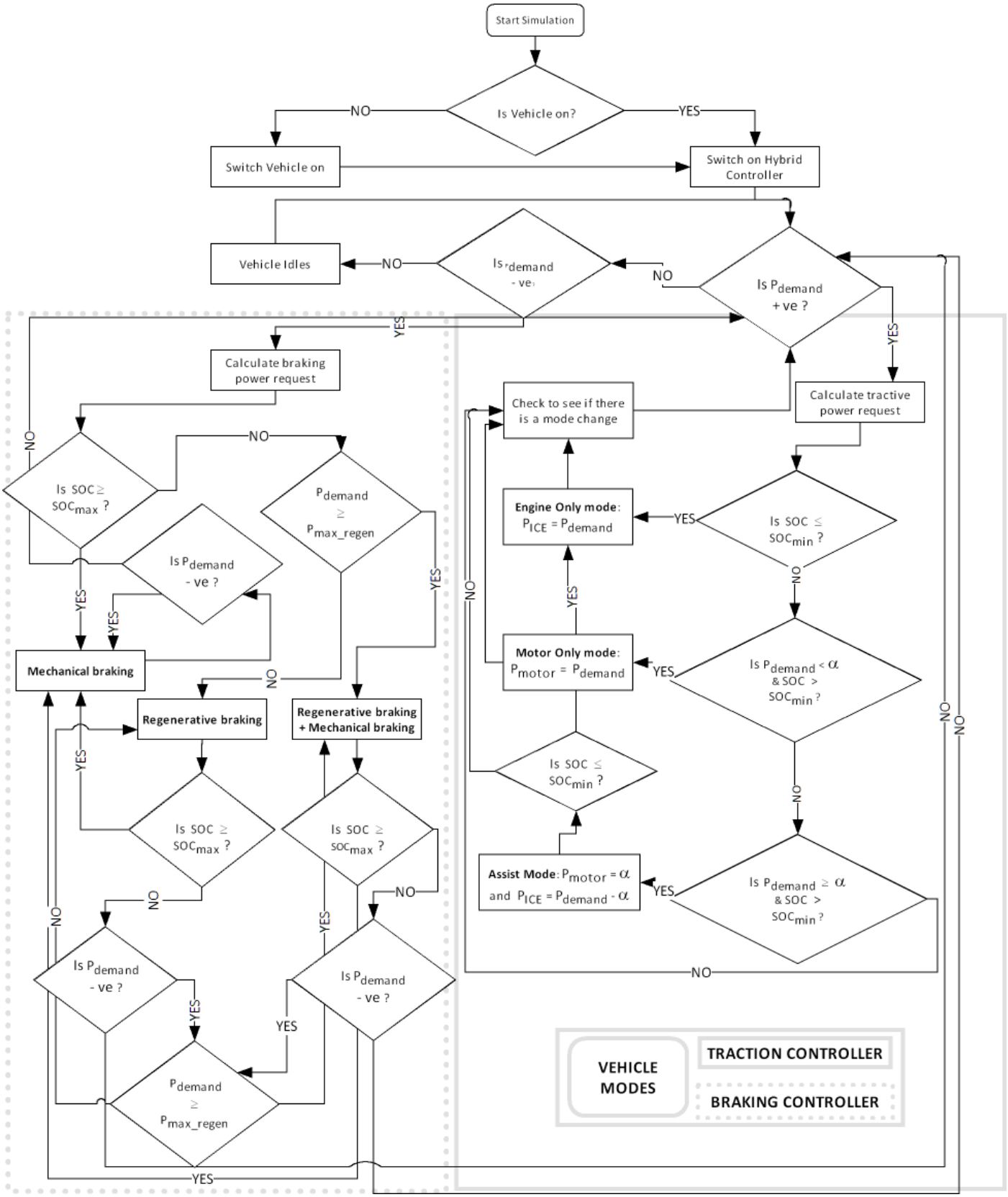

Figure 8: Heuristic control logic

3.2 Braking mode controller

The heuristic control logic shown in Figure 8, has been modelled in such a way that during braking, the electric motor speed is used via a look up table to estimate the maximum braking power capability of the electric motor at that instant "P_{max_regen}". The estimated value is then passed in to the controller where it is been used alongside the battery energy indicator (state of charge) thus to decide the appropriate mode of braking:-

If $P_{demand} < P_{max\_regen}$ & SOC < SOC_{max} : Regenerative braking only mode is selected.

During this mode:

$P_{motor} = P_{demand}$

If $P_{demand} \geq P_{max\_regen}$ & SOC < SOC_{max} : A combination of regenerative and mechanical braking mode is selected.

During this mode:

$P_{motor} = P_{max\_regen}$

$P_{mech\_brake} = P_{demand} - P_{max\_regen}$

If SOC ≥ SOC_{max} : Mechanical braking only mode is selected.

During this mode:

$P_{mech\_brake} = P_{demand}$

3.3 Traction mode controller

During the traction mode a "switch parameter" (α) is used alongside the battery state of charge to decide if the vehicle is to operate in any of the following modes:

(i) Engine only mode
(ii) Motor only mode
(iii) Assist mode

The "switch parameter" is determined outside the controller and can be computed thus:

$$\alpha = XP_{motor\_max} \quad (16)$$

Where X is the "motor power allocation factor" (0.1 – 1).

- *Maximum motor tractive power varies with motor speed and as such could be estimated via a look up table of (motor speed vs. maximum motor tractive power).*

Computing the "switch parameter" (α) using the method proposed in equation 16 implies that the "switch parameter" is a function of a known variable (maximum motor tractive power) and an unknown variable "X" (motor power allocation factor) which could be optimally tuned over different drive cycles. The method used in determining a suitable value of "motor power allocation factor" for the controller will be discussed in the next subsection. Before then, it is important to understand the role "α" plays in the tractive mode controller. These details will be discussed in the rest of this subsection.

The "switch parameter" (α) in this controller is an indication of the maximum level of power contribution the electric motor is allowed to make at any instant when the tractive mode is active.

During traction mode, the "switch parameter" (α) is used alongside the battery energy indicator (state of charge) thus to decide the appropriate power split between the electric motor and the internal combustion engine:-

If P_{demand} < α & SOC > SOC_{min} : Motor only mode is selected.

During this mode:

$P_{motor} = P_{demand}$

If P_{demand} ≥ α & SOC > SOC_{min} : Assist mode is selected.

During this mode:

$P_{motor} = \alpha$

$P_{ICE} = P_{demand} - \alpha$

If SOC ≤ SOC_{min} : Engine only mode is selected:

During this mode:

$P_{ICE} = P_{demand}$

- P_{ICE} *indicates the proportion of vehicle tractive power request handled by the ICE.*

3.4 Estimation of the motor power allocation factor "X"

In section 3.3, the relevance of the "switch parameter" (α) to the functionality of the proposed heuristic control strategy was outlined. This parameter as shown in equation

16 contains one known variable (maximum motor tractive power) and one unknown variable "X" (motor power allocation factor).

In order to estimate an appropriate value for the "motor power allocation factor" for this controller, a sensitivity analysis of its impact on cumulative fuel savings and battery state of charge was carried out over the NEDC, FTP72 and JAPAN1015 drive cycle as shown in Figure 9 - Figure 11. This analysis was made by simply running the controller simulations for all values of "motor power allocation factor" and noting the corresponding percentage of cumulative fuel savings (%), final battery state of charge (%) and cumulative motor tractive energy (MJ) value in each case. The noted values are then used to plot the graphs detailed in Figure 9 - Figure 11.

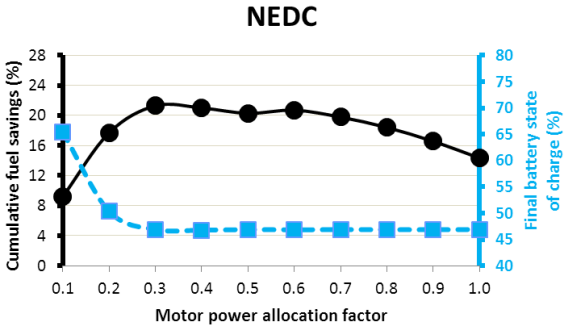

(a) Impact of motor power allocation factor on cumulative fuel savings and battery state of charge

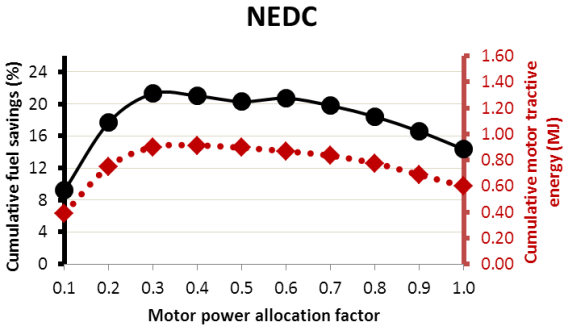

(b) Impact of motor power allocation factor on cumulative fuel savings and cumulative motor tractive energy

Figure 9: Motor power allocation factor analysis for the NEDC drive cycle

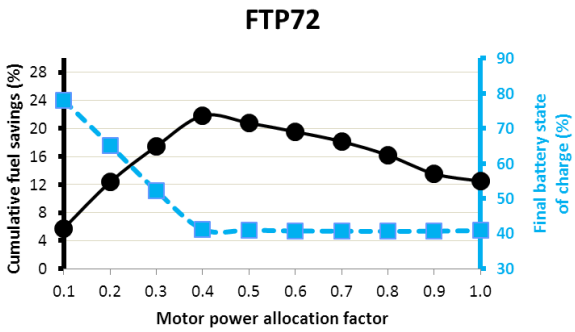

(a) Impact of motor power allocation factor on cumulative fuel savings and battery state of charge

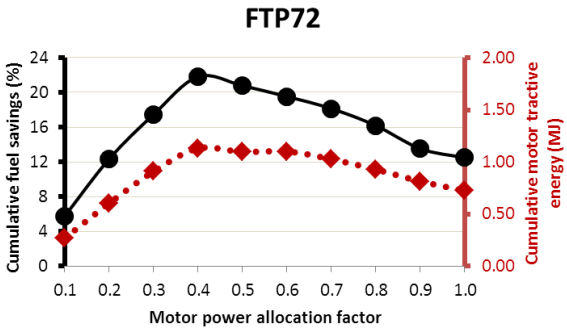

(b) Impact of motor power allocation factor on cumulative fuel savings and cumulative motor tractive energy

Figure 10: Motor power allocation factor analysis for the FTP72 drive cycle

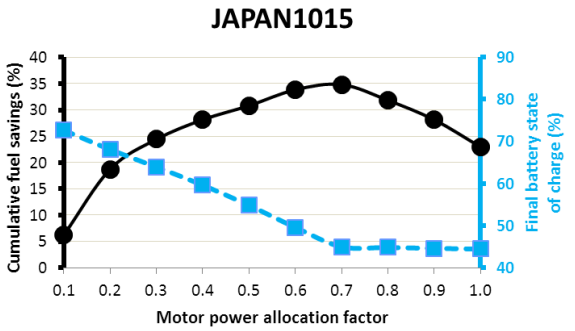

(a) Impact of motor power allocation factor on cumulative fuel savings and battery state of charge

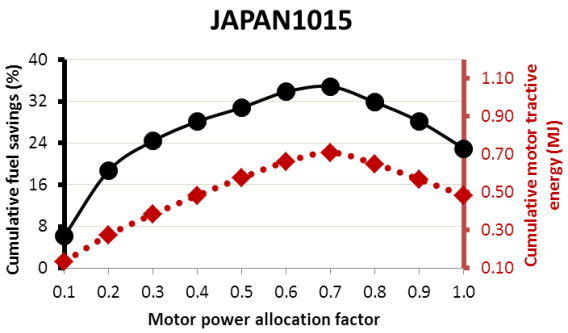

(b) Impact of motor power allocation factor on cumulative fuel savings and cumulative motor tractive energy

Figure 11: Motor power allocation factor analysis for the JAPAN1015 drive cycle

These drive cycles have been chosen to represent a range of driving scenarios. The NEDC and JAPAN1015 drive cycle simulates modal driving which is often characterized by low vehicle speed, low engine load and low exhaust gas temperature. Although these cycles are stylistic in nature and do not represent real world driving, it however offers the opportunity for hybridization potentials to be explored under idealized mild driving conditions. Conversely, the FTP72 drive cycle simulates real world transient driving patterns (characterized by rapid speed changes) which is very useful for assessing hybridization potentials under aggressive real world driving conditions [42]. A summary of the key characteristics that define the chosen drive cycles are detailed in Table 1.

Drive cycle type	% of time accelerating	% of time standing	% of time Spent Braking	Average positive acceleration (m/s^2)	Positive Kinetic energy (m/s^2)	Average driving speed (m/s)
NEDC	23.56	20.40	16.95	0.53	0.22	9.33
FTP72	31.90	13.81	19.80	0.43	4.31	8.78
JAPAN1015	29.55	26.06	22.58	0.37	4.17	6.31

Table 1: Drive cycle characteristics [43].

On all 3 drive cycles analysed, a decline in battery state of charge is observed for increased "motor power allocation factor". This trend stems directly from the fact that as the motor power allocation factor is increased, the magnitude of motor power contributed at each instant of engine assist also increases, thus leading to rapid instantaneous depletion in battery state of charge and a corresponding decrease in the final battery state of charge.

As shown in Figure 9(b), Figure 10(b) and Figure 11(b) for the NEDC, FTP72 and JAPAN1015 drive cycle respectively, an initial increase in "motor power allocation factor" corresponds to an increase in cumulative motor tractive energy and cumulative fuel savings. This trend is however reversed in each drive cycle once the peak cumulative motor tractive energy and peak cumulative fuel savings is reached, such that further increase in motor power allocation factor corresponds to a decrease in cumulative motor tractive energy and cumulative fuel savings. Saturation in instantaneous battery state of charge is believed to be responsible for the reversed trend observed in both cases. In this region, the rapid instantaneous depletion in battery state of charge associated with increased motor power allocation factor appears to be inhibitive to the overall motor tractive energy contribution; this happens due to fact that as the "motor power allocation factor" increases, the battery energy gets used up much quicker and earlier in the drive cycle and there is no battery energy left to facilitate further use of the electric motor for the rest of the drive cycle.

From Figure 9 - Figure 11 it could also be inferred that for each drive cycle, there exist a unique "motor power allocation factor" which simultaneously guarantees fuel savings and sustainability of battery state of charge over the entire drive cycle. A summary of the heuristic controller results under charge sustainability are detailed in Table 2 for each of the 3 drive cycles analysed.

Drive cycle type	Motor power allocation factor	Baseline cumulative fuel consumption (g)	Heuristic controller cumulative fuel consumption (g)	Cumulative fuel consumption savings (%)	Final battery state of charge (%)
NEDC	0.13	441.40	394.75	10.57	60.00
FTP72	0.24	476.80	407.27	14.58	
JAPAN1015	0.39	185.50	133.79	27.87	

Table 2: Heuristic controller results under charge sustainability

Estimating this unique "motor power allocation factor" for different driving scenarios in real time isn't however possible due to the iterative nature of the solution process. Despite this challenge, it is however possible to obtain a single tuned "motor power allocation factor" which will in real time guarantee some fuel savings, whilst still minimizing the difference between the Initial and final battery state of charge.

In order to obtain this single value, the following steps were undertaken:

1. For each "motor power allocation factor", combine the cumulative fuel savings (%) values from all 3 analysed drive cycles (NEDC, FTP72, JAPAN1015) and average them out.
2. For each "motor power allocation factor", combine the final battery state of charge values from all 3 analysed drive cycles and average them out.
3. Using the derived results, create the graph shown in Figure 12.

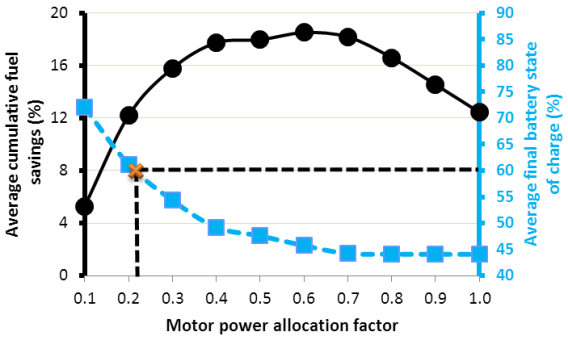

Figure 12: Impact of "motor power allocation factor" on average cumulative fuel consumption savings and average final battery state of charge

From Figure 12, the appropriate "motor power allocation factor" which is applicable in real time to the proposed controller is decided on the basis of final battery state charge sustainability to be 0.21.

4 CONTROL STRATEGY IMPLEMENTATION AND EVALUATION

In this section, the hybridization potentials of the proposed heuristic control strategy is accessed over the NEDC, FTP72 and JAPAN1015 drive cycle in real time. In order to achieve this potential, the "motor power allocation" factor of 0.21 which was estimated in section 3.4 is applied to the controller in real time.

Over the NEDC drive cycle, which represents a gentle urban driving pattern, the electric motor is found to carry out most of the braking events as detailed in Figure 13(b).

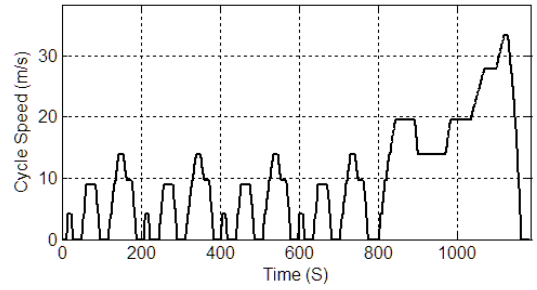

(a) NEDC drive cycle profile

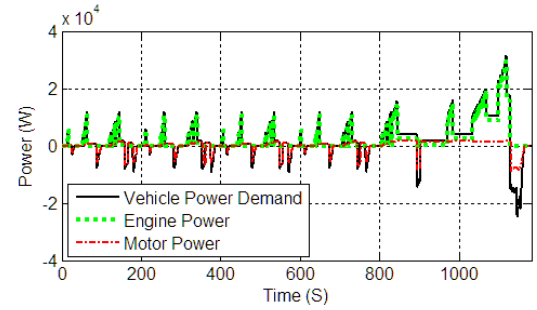

(b) Power split between electric motor and engine

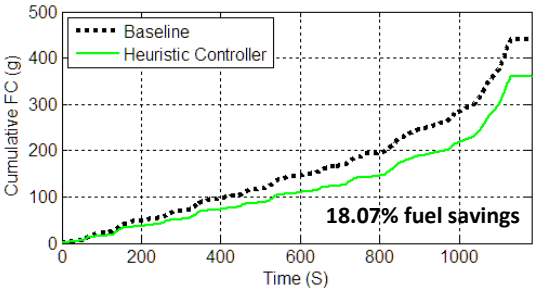

(c) Cumulative fuel consumption profile

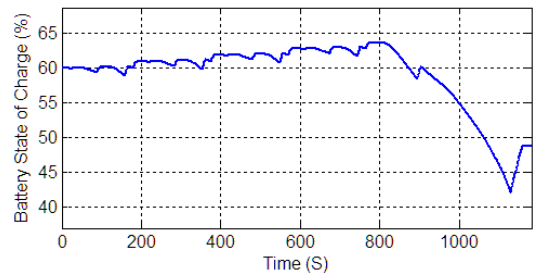

(d) Battery state of charge profile

Figure 13: Controller simulation results for NEDC drive cycle

Over the first 800 seconds of the NEDC drive cycle as shown in Figure 13(a), it is noted that the gentle braking characteristics of the NEDC drive cycle makes it possible to achieve a substantial amount of braking energy recovery as shown in Figure 13(d).

Owing much to braking energy recovery, 18.07% cumulative fuel savings were achieved over the entire cycle as shown in Figure 13(c), with a final battery state of charge of 48.87% as shown in Figure 13 (d).

In comparison to the NEDC, the JAPAN1015 drive cycle as shown in Figure 14(a) is a drive cycle which represents urban driving patterns although with larger percentage of idle time and low engine power requirement. Over the JAPAN1015 drive cycle, the electric motor was found to carry out most of braking events as shown in Figure 14(b).

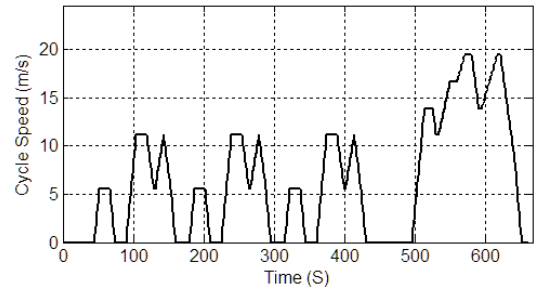

(a) JAPAN1015 drive cycle profile

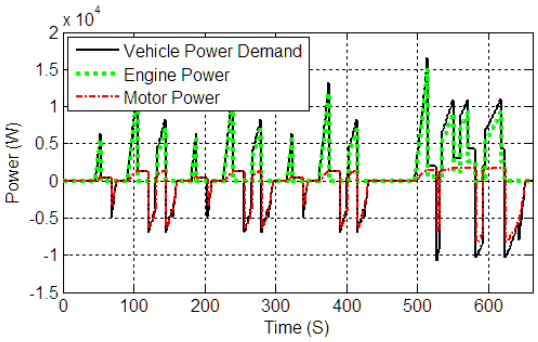

(b) Power split between electric motor and engine

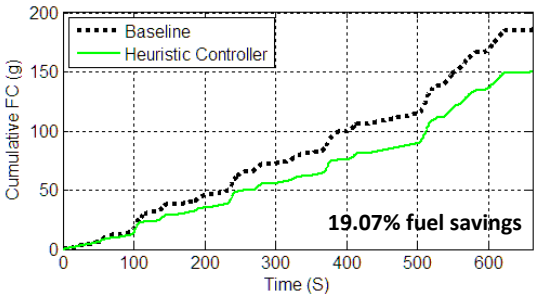

(c) Cumulative fuel consumption profile

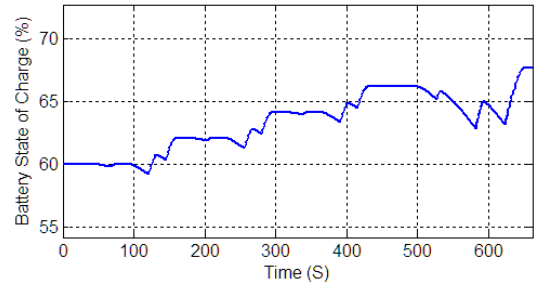

(d) Battery state of chare profile

Figure 14: Controller simulation results for JAPAN1015 drive cycle

The applied "motor power allocation factor" of 0.21 for the entire controller appeared to limit the tractive power contribution of the electric motor throughout the drive cycle. This resulted in more energy being captured than was utilized at the end of the cycle. Consequently, an energy surplus of 7.68% was realised on the final battery state of charge as shown in Figure 14(d). 19.07% cumulative fuel savings were realized at the end of the JAPAN1015 drive cycle as shown in Figure 14(c), with a final battery state of charge of 67.68% as shown in Figure 14(d).

The FTP72 drive cycle though more aggressive than the NEDC and JAPAN1015 drive cycles, offers lots of braking opportunities throughout the drive cycle as shown in Figure 15(a).

This makes it possible for the proposed heuristic controller to achieve a near balance between the energy going in and out of the battery via the electric motor (Figure 15(d)). Over this cycle 12.85% cumulative fuel savings were achieved with a final battery state of charge of 63.91%.

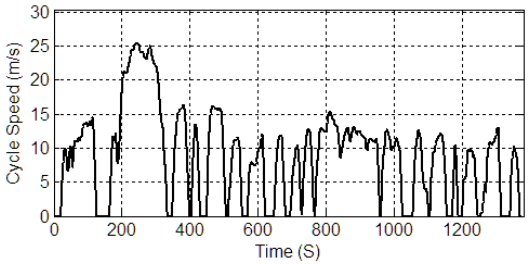

(a) FTP72 drive cycle profile

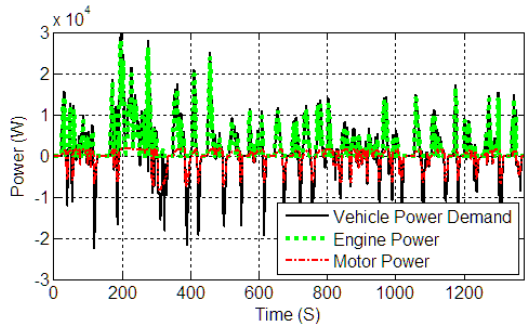

(b) Power split between electric motor and engine

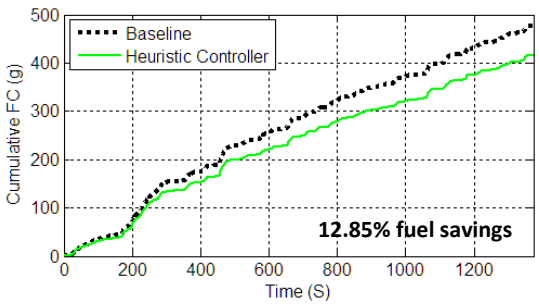

(c) Cumulative fuel consumption profile

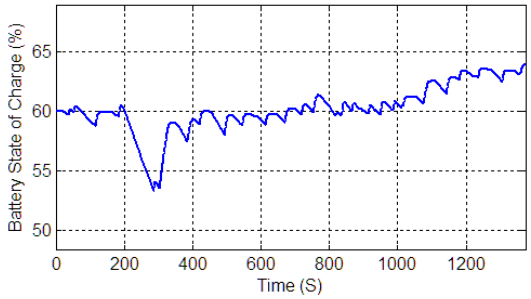

(d) Battery state of charge profile

Figure 15: Controller simulation results for FTP72 drive cycle

A summary of the fuel saving potentials derived from applying the proposed heuristic control strategy to different drive cycles in real time are detailed in Table 3.

Drive cycle type	Motor power allocation factor	Baseline cumulative fuel consumption (g)	Heuristic controller cumulative fuel consumption (g)	Cumulative fuel consumption savings (%)	Battery state of charge (%)
NEDC	0.21	441.40	361.65	18.07	48.87
FTP72		476.80	415.51	12.85	63.91
JAPAN1015		185.50	150.13	19.07	67.68

Table 3: Heuristic controller results with a "motor power allocation factor" of 0.21

5 DETERMINISTIC OPTIMAL CONTROL

In this section, dynamic programming optimal control algorithm is developed and used as the ultimate controller benchmark for our proposed heuristic control strategy under charge sustenance. Using rule extraction, the optimal control signals from dynamic programming are adapted to work in real time and the resultant suboptimal controller is further compared to our proposed heuristic controller.

5.1 HEV model simplification

Dynamic programming is well known to require computations which grow exponentially with the number of states and thus require a simpler vehicle model than the one presented in section 2. For the dynamic programming process, the HEV battery model presented in section 2.7 is simplified to a static equivalent circuit with input of motor mechanical power and output of battery state of charge as shown in equation 17.

$$SOC_{t+1} = SOC_t \pm \frac{V_{oc} - \sqrt{{V_{oc}}^2 - 4RP_{motor}\,\eta_{motor}\,\eta_{dis/chg}}}{2RQ} \qquad 17$$

Charing (+), Discharging (-).

To reduce the difference between the actual vehicle model and the simplified model, the same gear shift sequence as proposed in section 2.5 is applied during the dynamic programming process. The shift sequence is pre-calculated for each drive cycle and then applied during the dynamic programming process.

5.2 Dynamic programming problem formulation

In order to apply dynamic programming to solve HEV energy management problems, the problem needs to be set up in form of a cost function and a state transition function.

In the case of our HEV, the cost function could be expressed thus:-

$$C_{t+1} = \sum_{t=0}^{N-1} L(W_{ICE_t}, P_{motor_t}) \qquad 18$$

Where N is the time length of the driving cycle, and L is the instantaneous fuel consumption rate and C_{t+1} is the cost function (fuel consumption) to be minimized. W_{ICE} is the engine speed as previously derived in equation 8. P_{motor} is the vector of control variables.

The cost function formulated in equation 18 does not impose a charge sustaining policy and as such the optimization algorithm will tend to deplete the battery in order to attain minimal fuel consumption. Charge sustenance is imposed by adding a soft quadratic penalty to the overall cost function outlined in equation 18, such that the new cost function for the charge sustaining optimization problem becomes:-

$$C_{t+1} = \sum_{t=0}^{N-1} L(W_{ICE_t}, P_{motor_t}) + \emptyset(\mathrm{SOC(N)} - \mathrm{SOC}_f)^2 \qquad 19$$

Where SOC_f is the desired final state of charge at the end of the drive cycle and Ø is the weighting factor.

The aim of the optimization is to find the optimal input P_{motor} (motor mechanical power) which minimizes the total cost function "C_{t+1}" over the entire drive cycle.

The state transition function for this HEV is represented by equation 17 which is an indication of the battery state of charge.

Limitations in the operating range of the electric motor and battery means that constraints must be applied to the state (battery state of charge) and control policies (motor mechanical power) as shown below in order to ensure that they operate within their safe limits.

$$SOC_{min} \leq SOC \leq SOC_{max}$$

$$P_{motor\_min}(w_{motor}) \leq P_{motor} \leq P_{motor\_max}(w_{motor})$$

Constraints to the engine operating range are implemented inform of adjustments to the cost function during the dynamic programming routine as shown in Table 4.

Event	Fuel consumption cost	Reason
$P_{demand} > 0$ & $P_{motor} = P_{demand}$	0.12 g/s	Engine Idling
$P_{demand} = 0$	0.12 g/s	Engine Idling
$P_{demand} < 0$	0 g/s	Vehicle braking thus fuel has been cut off
$T_{ICE} > T_{ICE_{max}}$ $W_{ICE} > W_{ICE_{max}}$ $W_{ICE} < W_{ICE_{min}}$	Infinite cost	Infeasible operating area

Table 4: Cost adjustments during dynamic programming

5.3 Dynamic programming implementation

In order to find a solution to the HEV optimal control problem set up in section 5.2, the generic dynamic programming tool developed by Sundstrom *et al.* [44] was used.

This tool employs the backward recursive approach detailed below to find the optimal control policy (motor mechanical power) subject to the control constraints defined in section 5.2.

At step $N-1$

$$C^*_{N-1}(SOC(N-1)) = \min_{P_{motor_{N-1}}} \left[L(SOC(N-1), P_{motor}(N-1)) + \emptyset(SOC(N) - SOC_f)^2\right]$$

At step t for $0 \leq t \leq N-1$

$$C^*_t(SOC(t)) = \min_{P_{motor}(t)} \left[L(SOC(t), P_{motor}(t)) + C^*_{t+1}(SOC(t+1))\right]$$

N is the time length of the drive cycle.

6 HEURISTIC CONTROLLER PERFORMANCE BENCHMARK

6.1 Under charge sustenance

The optimal control problem set up in section 5 is solved over the NEDC, FTP72 and JAPAN1015 drive cycles. These results are used to benchmark the charge sustaining performance of our proposed heuristic controller as shown in Figure 16.

In comparison to the optimal controller, the heuristic controller though simpler in nature and less time consuming to implement, offers sensible fuel savings over the three cycles analysed.

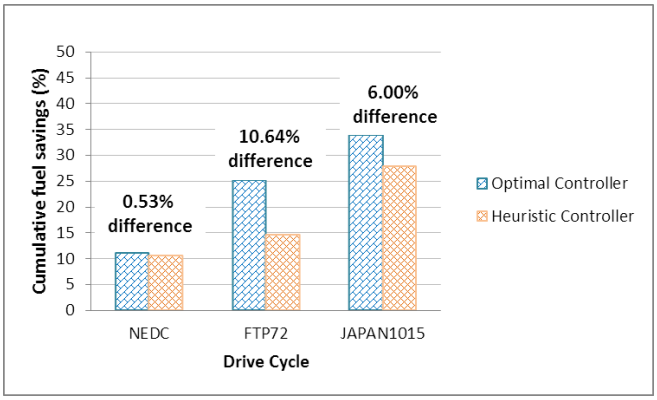

Figure 16: Comparison of optimal controller and proposed heuristic controller under charge sustenance

6.2 Under charge non-sustenance

Although the dynamic programming approach provides an optimal benchmark for other controllers, the resulting control policy is not implementable in real time due to the need for knowledge of prior vehicle power request. Nonetheless, analysing the resultant optimal control policies can provide some insights in to optimal rule extraction for real time implementation.

The derived suboptimal controller, though non charge sustaining, will prove useful as a comparison to the performance of our proposed heuristic controller in real time. In order to extract suboptimal control rules for real time implementation, we evaluate the engine power – speed operating points of all 3 drive cycles analysed as shown in Figure 17.

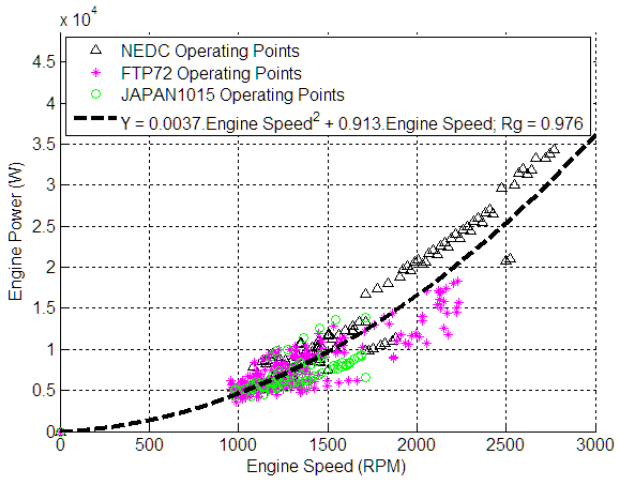

Figure 17: Optimal engine operating points for NEDC, FTP72 and JAPAN1015 drive cycles

The regression fit between the engine operating points: $Y = 0.00370\, W_{ICE}{}^2 + 0.913\, W_{ICE}$ is used thus to define the suboptimal control rules.

If $P_{demand} > Y \; and \; SOC > SOC_{min}$
$P_{motor} = P_{demand} - Y$
Else if $P_{demand} \leq Y \; and \; SOC > SOC_{min}$
$P_{motor} = P_{motor\_max}$

The real time performance of both the suboptimal controller and our proposed heuristic controller is analysed over the NEDC, FTP72 and JAPAN1015 drive cycle as shown in Table 5.

Drive cycle	Heuristic Controller		Suboptimal Controller	
	Final battery state of charge (%)	Cumulative fuel consumpton savings (%)	Final battery state of charge (%)	Cumulative fuel consumpton savings (%)
NEDC	48.87	18.07	46.89	16.58
FTP72	63.91	12.85	40.73	14.37
JAPAN1015	67.68	19.07	44.70	26.00

Table 5: Comparison of suboptimal controller and proposed heuristic controller under charge non sustenance

These results show the suboptimal controller to be massively charge depleting in all instances and in the case of the NEDC drive cycle, very inefficient. Over the NEDC drive cycle, it could be observed that the proposed heuristic controller out performs the suboptimal controller by using less battery energy to achieve more fuel savings.

7 IMPACT OF BRAKING PATTERNS ON KINETIC ENERGY RECOVERY

Whilst exploring the hybridization potentials of the proposed heuristic control strategy over different drive cycles in section 4, gentle braking patterns as in the case of the NEDC drive cycle (Figure 13) were found to promote energy recovery in to the battery. Sequel to this observation, this section aims to further investigate quantitatively using vehicle deceleration, the impact of braking patterns on kinetic energy recovery.

When braking a vehicle from speed of V_v(m/s) to a complete stop, the kinetic energy available for recovery can be characterised using equation 20 below.

$$E = \frac{1}{2} m V_v{}^2 \qquad 20$$

This implies that irrespective of the braking deceleration, kinetic energy available for capture remains constant for each "initial braking speed" as shown in Figure 18 below.

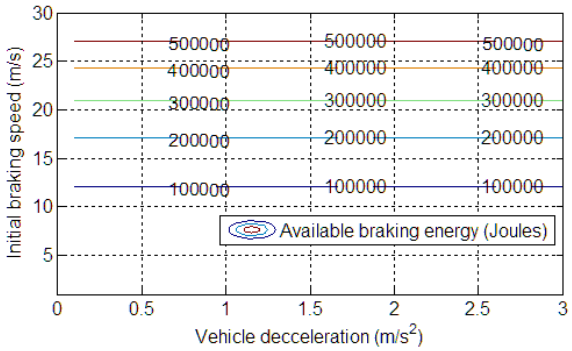

Figure 18: Available braking energy

With an objective of energy regeneration optimisation in mind, the imperative question then becomes: how best can braking be carried out so energy regeneration is optimised?

In order to address this problem, 5 braking patterns with different constant decelerations have been investigated as shown in Figure 19 below.

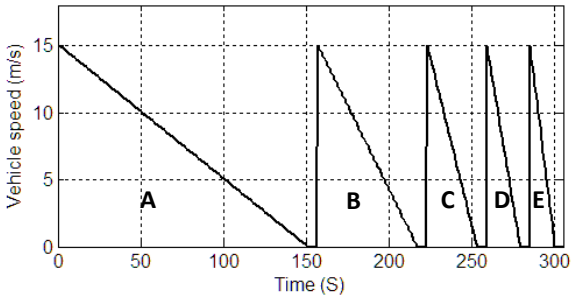

(a) Braking patterns

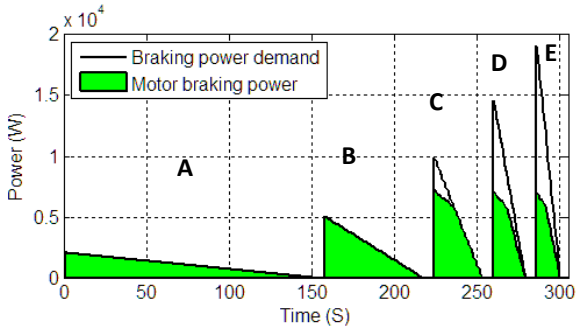

(b) Braking power distribution

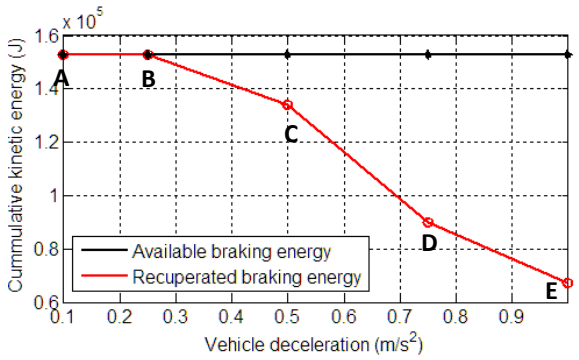

(c) Impact of vehicle deceleration on braking energy regeneration

Figure 19: Braking pattern analysis

The braking patterns considered as shown in Figure 19(a) represents vehicle braking from 15m/s to 0m/s under different constant rates of deceleration; A(0.10 m/s^2), B(0.25 m/s^2), C(0.50 m/s^2), D(0.75 m/s^2) and E(1.00 m/s^2). This implies that the kinetic energy available in each case is the same as shown in Figure 19(c). Although, in reality cars don't brake under constant deceleration, representing vehicle braking patterns in this manner is mainly for simplification reasons. This study also assumes an ideal regenerative braking system; as such the only impedance to energy regeneration is the instantaneous power limit of the electric motor which varies with motor speed.

As shown in Figure 19(c), an increase in vehicle deceleration beyond 0.25m/s^2, correspond to a decrease in kinetic energy regeneration by the electric motor. This trend could be understood by looking at Figure 19(b). According to this figure, as vehicle deceleration increases, the braking time significantly reduces, however the instantaneous braking power demand increases significantly. Owning to limitations in the instantaneous braking power of the electric motor, increased energy loss is observed as vehicle deceleration increases.

The study presented in Figure 19 is further expanded in Figure 20 to feature a range of constant vehicle decelerations occurring at different initial vehicle braking speeds. Observations from this graph further confirm inferences made in Figure 19, where for each initial vehicle braking speed, the percentage of kinetic energy regenerated decreases with increased vehicle deceleration. As shown in Figure 20, for most initial vehicle braking speeds, optimisation of braking energy regeneration is possible if braking occurs at deceleration rates below 0.5m/s^2.

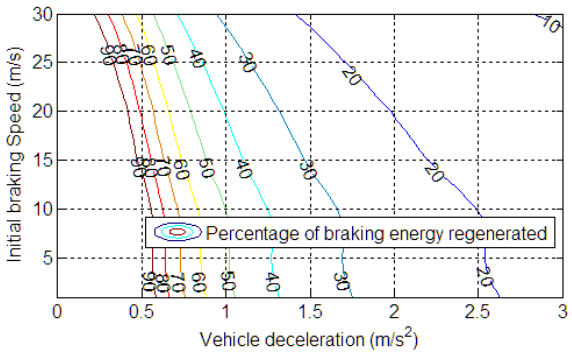

Figure 20: Impact of vehicle deceleration on braking energy regeneration

8 CONCLUSIONS AND FURTHER WORK

This paper presents detailed longitudinal quasi-static modelling and validation of a parallel HEV. Using the validated model, further analysis was carried out over the NEDC drive cycle to investigate the effect of an early gear upshift on cumulative fuel consumption. Results from this analysis showed that gear upshift at a lower engine speed saves more fuel than carrying out the same manoeuvre at a higher engine speed. However, legislative tests define gear change time in many cases.

A simple but effective heuristic control strategy which uses a tuneable parameter "motor power allocation factor" to decide the tractive power split between the electric motor and the internal combustion engine is modelled and applied to the parallel HEV.

Analysis on the impact of "motor power allocation factor" on fuel saving potentials of the vehicle showed that there exist a unique value of "motor power allocation factor" which guarantees both fuel savings and charge sustainability for each of the drive cycles analysed. This value however cannot be determined in real time, due to the iterative nature of the solution process. Results

obtained from this analysis were used to select 0.21 as an appropriate value of "motor power allocation factor" which is applicable in real time to the controller.

Using a "motor power allocation factor" of 0.21, the modelled heuristic control strategy was applied in real time over a range of drive cycles. Hybridization fuel saving potentials of approximately 18.07%, 12.85%, and 19.07% were observed over the NEDC, FTP72 and JAPAN1015 drive cycles respectively. In comparison to a suboptimal controller whose control signals were derived from dynamic programming optimal control, our proposed strategy was found to be outperforming, in that impressive real time fuel savings were achieved without much penalty to the final battery state of charge.

Gentle braking patterns were found to facilitate significant kinetic energy recovery by the electric motor. Vehicle deceleration less than 0.5m/s^2 was also found to optimize braking energy regeneration.

Despite the fuel saving potentials of the proposed control strategy, the control approach used is unable to guarantee optimality of the cost function (fuel consumption). It is also unable to satisfy in real time, final integral constraints e.g. (sustainability of the battery state of charge at end of the drive cycle). As a result, future research studies will aim to develop a look ahead heuristic control strategy which will be able to estimate the vehicle's speed a priori and iteratively tune the "motor power allocation factor" of the controller offline, such that fuel savings and charge sustainability could be simultaneously achieved in real time. Experimental validation of the fuel savings reported in this paper, will also form a major part of our future research.

ACKNOWLEDGEMENT

The authors would like to thank Ashwoods Automotive and Perm motor Germany for providing us with the engine and electric motor experimental test data used for this research.

NOMENCLATURE

General Nomenclature

NEDC	New European Drive Cycle
FTP	Federal Test Procedure
HEV	Hybrid Electric Vehicle
FC	Fuel Consumption
J	Joule
kJ	Kilojoule
MJ	Megajoule
NOx	Oxides of Nitrogen
HC	Hydrocarbons
CO	Carbon Monoxide
ICE	Internal Combustion Engine

Driver Model

T_{extra}	Extra wheel torque needed for the vehicle to achieve the requested vehicle speed (Nm)
F_{extra}	Extra tractive force needed for the vehicle to achieve the requested vehicle speed (N).
K_p	Proportional Gain
K_i	Integral Gain
K_d	Differential Gain
V_c	Cycle Speed (m/s)
V_v	Vehicle Speed (m/s)

Vehicle Dynamics and Engine

F_{grade}	Resistance force by grade (N)
F_{aero}	Aerodynamic drag force (N)
$F_{rolling}$	Rolling resistance force (N)
m	Effective mass of vehicle (Kg)
$\frac{dV_v}{dt}$	Acceleration (m/s^2)
Eff	Drive train efficiency
FDR	Final drive ratio
G_E	Engine gear ratio
G_M	Motor gear ratio
T_{ICE}	Tractive torque from internal combustion engine (Nm)
$T_{ICE\,max}$	Maximum tractive torque from internal combustion engine (Nm)
W_{ICE}	Engine speed (RPM)
P_{ICE}	Engine Power (W)
W_{wheel}	Wheel Speed (RPM)
μ	Coefficient of rolling resistance
N_c	Normal load acting on the centre of the rolling wheel (N)
R_w	Radius of rolling wheels (m)
$T_{rolling}$	Rolling resistance moment (Nm)
ρ	Air density (kg/m^3)
A_f	Vehicle frontal area (m^2)

C_d	Aerodynamic drag coefficient
V_a	Velocity of the air (m/s)
g	Gravitational constant (m/s^2)
β	Inclined vehicle angle
P_{mech_brake}	Mechanical brake
R_g	Correlation coefficient

Electrical Motor

P_{motor}	Motor mechanical power (W)
$P_{electric}$	Motor electrical power (W)
η_{motor}	Motor efficiency function of speed and torque
$P_{\max\_regen}$	Maximum motor regenerative power
P_{motor_max}	Maximum motor tractive power
w_{motor}	Motor speed (RPM)
T_{motor}	Motor Torque (Nm)

Electrical Battery

$P_{battery}$	Battery power (W)
V_{batt}	Battery voltage (V)
V_{oc}	Battery open circuit voltage (V)
R	Battery Resistance (Ohms)
SOC_{t+1}	Future battery state of charge
SOC_t	Present state of charge
SOC_{min}	Minimum battery state of charge
SOC_{max}	Maximum battery state of charge
t	Present simulation (s)
t+1	Future simulation time (s)
I	Battery current (A)
Q	Battery capacity (Ah)
η_{dis}	Battery discharge efficiency
η_{chg}	Battery charge efficiency

REFERENCES

[1] Brahma A, Guezennec Y, Rizzoni G. Dynamic optimization of mechanical/electrical power flow in parallel hybrid electric vehicles: Proc. of 5th Int. Symposium in Advanced Vehicle Control, Ann Arbor, MI; 2000.

[2] Schouten NJ, Salman MA, Kheir NA. Fuzzy logic control for parallel hybrid vehicles. IEEE Transaction on Control Systems Technology. 2002;vol. 10, 460.

[3] Delprat S, Lauber J, Guerra TM. Control of a parallel hybrid powertrain: optimal control: IEEE Transactions on Vehicular Technology; 2004.

[4] Genta G. Motor Vehicle Dynamics: Modelling and Simulation World Scientific Pub Co. Inc. Singapore; 1997.

[5] Millo F, Rolando L, Andreata M. Numerical Simulation for Vehicle Powertrain Development: SBN: 978-953-307-389-7 In book: Numerical Analysis - Theory and Application; 2011.

[6] Guzzella L, Sciarretta A. Vehicle Propulsion Systems: Introduction to Modelling and Optimization: Springer: 9783642094156; Berlin 2007.

[7] Vassallo A, Cipolla G, Mallamo F. Transient Correction of Diesel Engine Steady-State Emissions and Fuel Consumption Maps for Vehicle Performance Simulation. Aachener Kolloquim Fahrzeug und Motorentechnik, Aachen, Germany 2007.

[8] Pettiti M, Pilo L, Millo F. Developement of a new mean value model for the analysis of turbolag phenomena in automotive diesel engines. SAE Technical paper; 2007-01-1301; 2007.

[9] Keribar R, Ciesla C, Morel T. Engine/Powertrain/Vehicle Modeling Tool Applicable to all Stages of the Design Process: SAE Technical Paper 2000-01-0934; 2000.

[10] Morel T, Keribar R, Leonard A. Virtual Engine/Powertrain/Vehicle Simulation Tool Solves Complex Interacting System Issues: SAE Technical Paper 2003-01-0372; 2003.

[11] Brahma A, Guezennec Y, Rizzoni G. Optimal energy management in series hybrid electric vehicles. Proceedings of the American Control Conference. 2000.

[12] Back M, Simons M, Kirschaum F, Krebs V. Predictive control of drivetrains. in Proc IFAC 15th Triennial World Congress, Barcelona, Spain. 2002.

[13] Lin C-C, Peng H, Grizzle JW, Kang J-M. Power management strategy for a parallel hybrid electric truck. IEEE Trans Contr Syst Technol. 2003;vol. 11, no. 6:pp. 839–49.

[14] Arsie I, Graziosi M, Pianese C, Rizzo G, Sorrentino M. Optimization of supervisory control strategy for parallel

hybrid vehicle with provisional load estimate. in Proc 7th Int Symp Adv Vehicle Control (AVEC), Arnhem, The Netherlands. 2004.

[15] Lin C, Kang J, Grizzle JW, Peng H. Energy Management Strategy for a Parallel Hybrid Electric Truck. Proceedings of the 2001 American Control Conference, Arlington, VA. 2001:pp.2878-83.

[16] O'Keefe MP, Markel T. Dynamic programming applied to investigate energy management strategies for a plug-in HEV. National Renewable Energy Laboratory, Golden, CO. 2006;Report No. NREL/CP- 540-40376.

[17] Gong Q, Li Y, Peng Z-R. Trip-based optimal power management of plug-in hybrid electric vehicles. IEEE Trans Veh Technol. 2008;vol. 57, no. 11:pp. 3393–401.

[18] Paganelli G, Delprat S, Guerra TM, Rimaux J, Santin JJ. Equivalent consumption minimization strategy for parallel hybrid powertrains. In Proc IEEE 55th Vehicular Technology Conference. 2002;volume 4:pages 2076–81.

[19] Pisu P, Rizzoni G. A comparative study of supervisory control strategies for hybrid electric vehicles. IEEE Trans on Control SystemsTechnology. 2007;vol. 15(3):pg. 506–18.

[20] Kleimaier A, Schr¨oder D. An approach for the online optimized control of a hybrid powertrain. Proceedings of 7th International Workshop Advanced on Motion Control. 2002:pp. 215–20.

[21] Rizzoni G, Pisu P, Calo E. Control strategies for parallel hybrid electric vehicles. Proceedings of IFAC Symposium on Advanced Automotive Control. 2004:pp. 508–13.

[22] Sciarretta A, Back M, Guzzella L. Optimal control of parallel hybrid electric vehicles. IEEE Transactions On Control Systems Technology. 2004;vol. 12(3).

[23] Delprat S, Guerra TM, Rimaux J. Optimal Control of a Parallel Powertain: From Global Optimization to Real Time Control Strategy. Proc of the 18th Electric Vehicle Symposium, EVS18. 2001.

[24] Kim N, Cha S, Peng H. Optimal Control of Hybrid Electric Vehicles Based on Pontryagin's Minimum Principle. IEEE TRANSACTIONS ON CONTROL SYSTEMS TECHNOLOGY. 2011;VOL. 19, NO. 5.

[25] Musardo C, Rizzo G, Staccia B. A-ECMS: An adaptive algorithm for hybrid electric vehicle energy management. In Proc Decision and Control Conference and European Control Conference. 2005:pages 1816–23.

[26] Onori S, L S, Rizzo G. Adaptive equivalent consumption minimization strategy for hevs. In 3rd Annual Dynamic Systems and Control Conference, Cambridge, MA. 2010.

[27] Sciarretta A, Guzzella L, Back M. A real-time optimal control strategy for parallel hybrid vehicles with on-board estimation of control parameters. In Proc IFAC Symposium on Advances Automotive Control, Salerno, Italy. 2004:pages 502–7.

[28] Guzzella L, Sciarretta A. Vehicle Propulsion Systems. Springer; 2005.

[29] Baumann BM, Washington G, Glenn BC, Rizzoni G. Mechatronic design and control of hybrid electric vehicles. IEEE/ASME Trans Mechatronics. 2000;vol. 5:pp. 58–72.

[30] Powell BK, Bailey KE, Cikanek SR. Dynamic modeling and control of hybrid electric vehicle powertrain systems. IEEE Control Syst Mag. 1998;vol. 18:pp. 17–33.

[31] Rizoulis D, Burl J, Beard J. Control strategies for a series-parallel hybrid electric vehicle. SAE, Warrendale, PA. 2001;Paper No. 2001-01-1354.

[32] Sharer PB, Rousseau A, Karbowski D, Pagerit S. Plug-in hybrid electric vehicle control strategy: Comparison between EV and charge-depleting options. SAE, Warrendale, PA. 2008;Paper No. 2008-01-0460.

[33] Rousseau A, Pagerit S, Gao D. Plug-in hybrid electric vehicle control strategy parameter optimization. Electric Veh Symp-23, Anaheim, CA2007.

[34] Schouten NJ, Salman MA, Kheir NA. Energy management strategies for parallel hybrid vehicles using fuzzy logic. Control Engineering Practice. 2003;vol. 11:pp. 171-7.

[35] Poursamad A, Montazeri M. Design of genetic-fuzzy control strategy for parallel hybrid electric vehicles. Control Engineering Practice. 2008;vol. 16:pp. 861-73.

[36] Rajagopalan A, Washington G. Intelligent control of hybrid electric vehicles using GPS information. Future Car Congress. 2002.

[37] Wong JY. Theory of Ground Vehicles: Third edition, United States of America, John Wiley & Sons. Inc; 2001.
[38] Ehsani M, Gao Y, Gay SE. Modern Electric, Hybrid Electric, and Fuel Cell Vehicles Fundamentals, Theory, and Design: Taylor & Francis Group; 2005.

[39] Jalil N, Kheir NA, Salman M. A Rule -Based energy management Strategy for a Series Hybrid Vehicle: Proceeding of American Control Conference; 1997.

[40] André M, Hickman J, Hassel D. Driving cycles for emission measurements under European conditions: SAE congress, Feb. 27 - March 2, 1995 Detroit, USA, SAE paper 950926, Warrendale, USA; 1995.

[41] Andre JM, lacour S, Hugot M. Impact of the gearshift strategy on emissions measurement: Artemis 3142 report: Report n° LTE 0307; 2003.

[42] DieselNet. Emissions Test Cycle: [Online] http://www.dieselnet.com/standards/cycles/; 2012.

[43] Barlow T, Latham S, McCrae I. A reference book of driving cycles for use in the measurement of road vehicles emissions: Department for Transport, Clearner Fuels & Vehicles; 2009.

[44] Sundstrom O, Guzzella L. A generic dynamic programming Matlab function. Control Applications, (CCA) & Intelligent Control, (ISIC), 2009 IEEE2009. p. 1625-30.

APPENDICES

Appendix 1: Vehicle modelling data

Vehicle Type	Light Commercial	
Fuel	Diesel	
Engine	1.6HDi 90hp	
Transmission	Gear 1	11/38
	Gear 2	15/28
	Gear 3	32/37
	Gear 4	45/37
	Gear 5	50/33

Vehicle Parameters

Wheel radius	0.307 meters
Drag Coefficient	0.35
Rolling Resistance	0.001
Vehicle mass	1360 Kg
Final drive ratio	4.2941
Car frontal area	$2m^2$
Drive train efficiency	1
Maximum Engine Speed	6500 RPM

Battery Parameters

Battery Cell Composition	Lithium Ion Phosphate
Battery Capacity	16 Ampere hours
Battery Resistance	0.024 Ohms
Minimum State of Charge	40%
Maximum State of Charge	80%
Battery open circuit voltage	60V

Electric Motor Parameters

Motor Manufacturer	Perm Motor Germany
Motor type	Brushless DC motor
Motor model	PMS 120
Max Motor torque	42 Nm
Max Motor Speed	4500 RPM
Motor Gear Ratio	1.178